BOOST BRIDGE AUDIO AMPLIFIER

Milan Prokin
Faculty of Electrical Engineering
Bulevar Revolucije 73, 11120 Belgrade, Yugoslavia
E-mail: proka@el.etf.bg.ac.yu

Abstract - The main difference in topology of a boost bridge amplifier and state-of-the-art class-D amplifier is in the connection of a loudspeaker between a power supply and a switching bridge. The boost bridge amplifier provides four times higher peak power at the loudspeaker than the power, which can be achieved by a class-D amplifier from the same power supply. Total harmonic distortion and amplifier efficiency are appropriate to a class-D amplifier, while power supply noise rejection is increased, on the expense of slightly increased loudspeaker dissipation.

1. Introduction

The basic problem in all state-of-the-art linear audio amplifiers in classes A, B and AB is the heat generation and low efficiency during amplification of music [1], requiring high power consumption from the power supply, which is of specific interest for battery supplied devices such as those in cars, mobile phones, portable computers, radios, cassette and CD players. This problem is successfully solved by a class-D amplifier (CDA) topology [2,3,4], in case of a single voice coil loudspeaker (Figures 1 and 2). Dual voice coil (DVC) loudspeaker can also be connected to a CDA, according to [5].

The input LC filter is usually implemented between the power supply and the switching bridge. The switching bridge output is connected to the loudspeaker through the output LC filter. The switching bridge operation is controlled by the pulse-width modulated control signals PWM. The pulse-width modulator can be made using the generator of a reference triangular or a sawtooth voltage and a comparator, which compares the said reference voltage with an input voltage to be modulated. The modulator can also be made of a counter in which digital words, appropriate to the binary value of input voltage samples, are written.

The input LC filter of a CDA, used to reduce injection of conducted EMI noise from the switching bridge into the cable connecting the power supply requires bulky components, whereby the price and the dimensions of CDA are increased. Furthermore, the design of such input LC filter requires special attention due to the mutual interaction between its output impedance and the input impedance of the switching bridge, in order to avoid voltage oscillations at the switching bridge [6]. The switching bridge draws pulsed current from the input LC filter, generating accordingly high level of conducted and radiated EMI noise, especially in the case of long cables between the power supply and the input LC filter.

The output LC filter of a CDA, used for the reconstruction of an analog signal from the pulse-width modulated signal at the output of the switching bridge, requires a large number of components of significant size, whereby the price and the dimensions of CDA are considerably increased. An interesting solution for this problem, describing active ripple cancellation filter is described in [7].

From early days of CDA development until now, various authors tried to increase the output power delivered by the power supply using the same loudspeaker impedance. A state-of-the-art high-power amplifier consisting of a boost converter connected to a CDA, as well as push-pull switching power amplifier made of two bidirectional Ćuk switching power supplies, are described in [8,9,10]. Unfortunately, such amplifier requires very small inductors and capacitors for the correct reproduction of high audio frequencies, leading to the increased current ripple through all switches and the increased output voltage ripple, significantly reducing amplifier efficiency. Furthermore, without modulation signal, voltages across switches reach twice the value of the power supply voltage, while

Contributed Paper
Manuscript received March 6, 2001

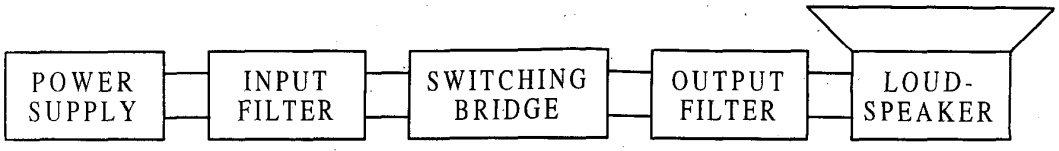

Figure 1 Block diagram of a state-of-the-art class-D amplifier

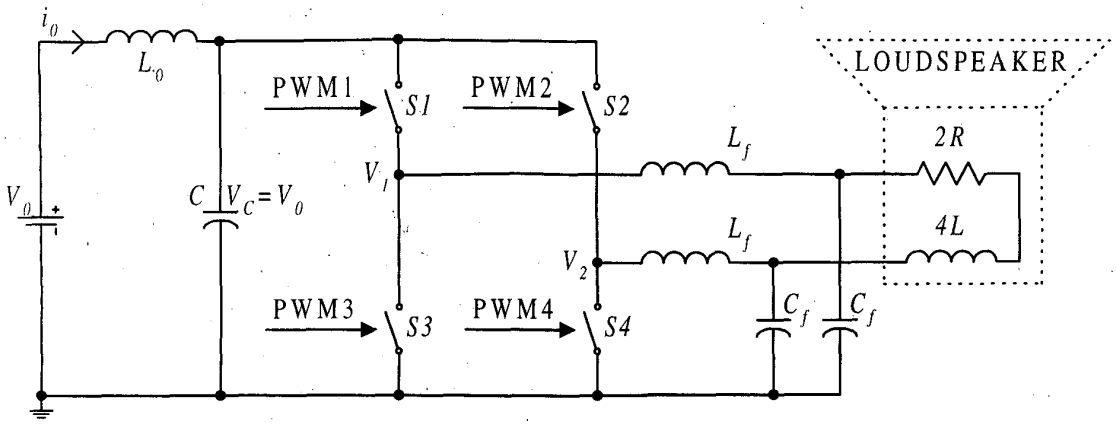

Figure 2 Schematic diagram of a state-of-the-art class-D amplifier

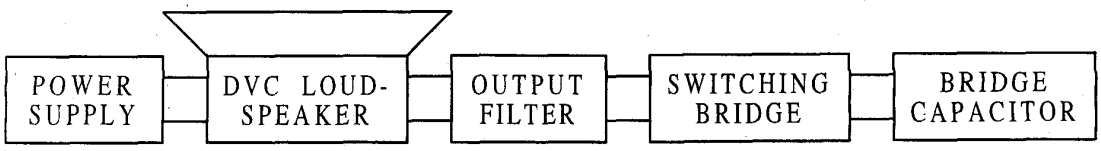

Figure 3 Block diagram of a novel boost bridge amplifier

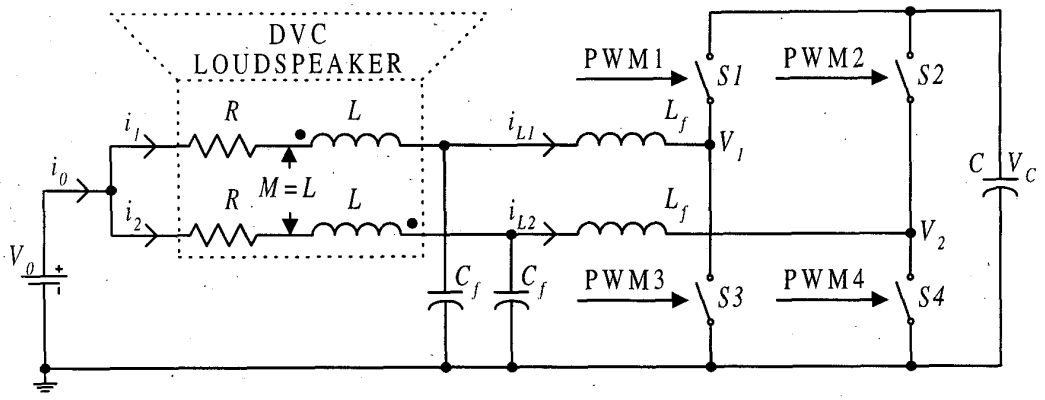

Figure 4 Schematic diagram of a novel boost bridge amplifier

during operation they could reach several times the value of the power supply voltage, which requires switches with high breakthrough voltage, together with very complex and accurate feedback based on sensing both currents through the input inductors and the voltages across the output capacitors.

2. BBA operation

Novel boost bridge amplifier (BBA) topology provides DVC loudspeaker connection BETWEEN the power supply and the output filter (Figures 3 and 4), which is completely opposite to the CDA case. The switching bridge voltage is provided by the bridge capacitor. Thus, BBA topology can completely eliminate the input filter.

The switching bridge operation is controlled by the pulse-width modulated control signals PWM1, PWM2, PWM3 and PWM4, which are typically counter phased for the switches connected to the same loudspeaker's phase and shifted for 180 electrical degrees between phases. In other words, signals PWM1 and PWM4 are active in the same time interval, while PWM2 and PWM3 are inactive, and vice versa, which is the most often used modulation for a CDA. Any controlled semiconductor device can perform role of a switch, such as MOSFET, IGBT, bipolar transistor or MCT, depending on the switching frequency and required power.

The inductances of both phases are coupled in most commercially available DVC loudspeakers. Power supply current i_0 is divided into two identical DC phase currents, which fluxes cancel each other according to the reference markers shown. Thus the summary DC flux equals zero, so these DC phase currents do not affect the behavior of the magnetic material inside the loudspeaker. The average force generated by mentioned DC phase currents is also cancelled to zero, which is obvious from both simulated short-scale and large-scale timing diagrams in Figures 5 and 6, respectively, made for $C = 100\mu F$ and power supply voltage of 14.4V, usual in car audio.

However, the modulated AC phase currents have opposite directions regarding the power supply, so their fluxes will add according to the reference markers shown. The force moving the voice-coil is proportional to the modulated "force" AC current i_f, which is produced by subtracting modulated AC phase currents, appropriately to both short-scale and large-scale timing diagrams in Figures 5 and 6, respectively.

A special feature of the BBA is practical insensitivity to the variations of the power supply voltage, which produce identical currents in symmetrical phases of the loudspeaker, so their fluxes and forces cancel each other.

Another special feature of the BBA is practical insensitivity to the variations of the bridge capacitor voltage, which produce identical currents in symmetrical phases of the loudspeaker, so their fluxes and forces cancel each other.

The output LC filter, connected between each phase of the loudspeaker and the appropriate output of the switching bridge, additionally filters current through the loudspeaker and provides necessary inductance for the voltage doubling operation. The output LC filter is preferably 2^{nd} order filter consisting of a filtering inductor and a capacitor per each phase, or 4^{th} order filter consisting of two filtering inductors and two filtering capacitors per each phase.

If necessary, additional attenuation of conducted EMI noise over a cable connecting the power supply and the loudspeaker can be made using an additional input LC filter. Although the same number of components will be utilized in such filter as in an input LC filter of the CDA, the values of both filtering elements in the input filter inside the BBA are several orders of magnitude less, because the current ripple, passing through the loudspeaker inside the BBA, is several orders of magnitude less than the current ripple passing through the switching bridge of the CDA.

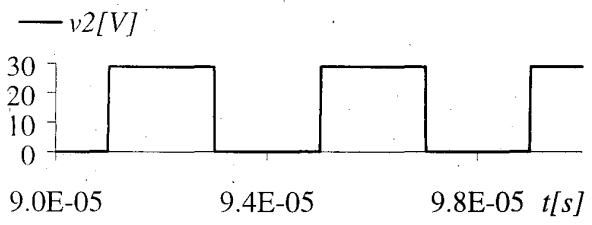

(a) V_2 output voltage

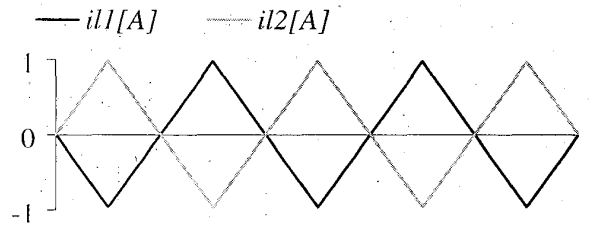

(b) i_{L1} and i_{L2} inductor's currents

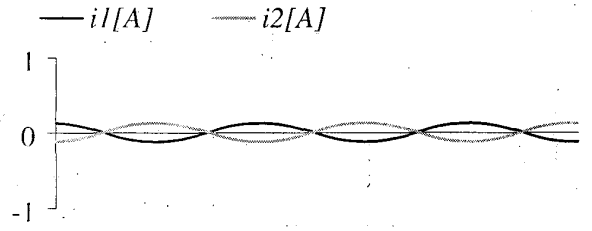

(c) i_1 and i_2 phase currents

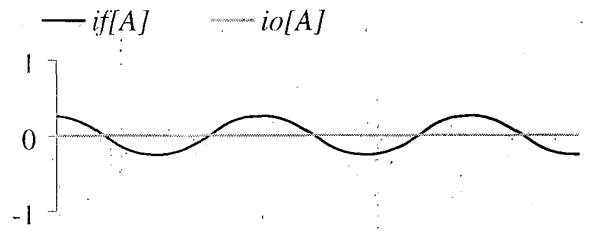

(d) i_f force and i_0 power supply currents

Figure 5 BBA idle timing diagrams

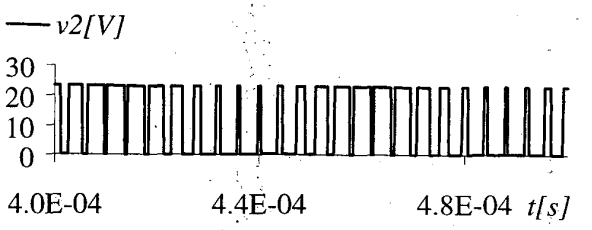

(a) V_2 output voltage

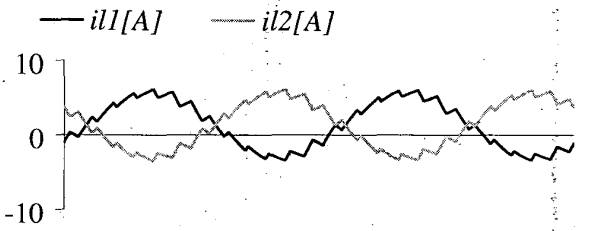

(b) i_{L1} and i_{L2} inductor's currents

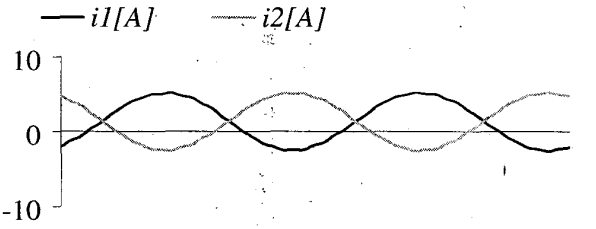

(c) i_1 and i_2 phase currents

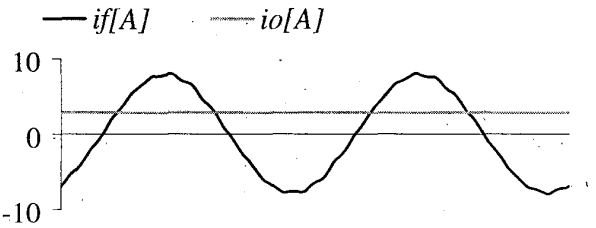

(d) i_f force and i_0 power supply currents

Figure 6 BBA sine wave timing diagrams

3. BBA steady-state analysis

The steady-state approximate equations describing the operation of the BBA are derived based on the following hypothesises:

- DVC loudspeaker is treated as a resistive load without back electromotive force;
- symmetrical load and/or mutually coupled load's phases;
- opposite phase wiring direction;
- negligible ripple of phase currents;
- negligible ripple of the bridge capacitor voltage;
- pulse-width modulated synchronous half-bridge switches per each phase;
- phase modulation signals with angular frequency ω, order of magnitude less than the cut-off frequency of the output LC filter;
- phase modulation signals shifted in time for 180 electrical degrees; and
- only switch conduction loss is calculated.

The crest factor CF as a ratio of maximum peak power to rms power expressed in dB, is a very important parameter in the field of audio power amplifiers. The crest factor for a sine wave signal is only 3.01dB; i.e. the peak power is only 2 times higher than the rms power. The analysis of various musical genres, from classical, pop, rock to jazz, shows a variation in crest factor from a minimum of 11dB for pop and rock to a maximum of 21dB for some classical or jazz music, which corresponds to a ratio of peak power to rms power from the minimum of 11.6 to the maximum of 126. In audio application it could be assumed that the average crest factor is about 15dB, i.e. 31.6 times for the majority of the musical content [11].

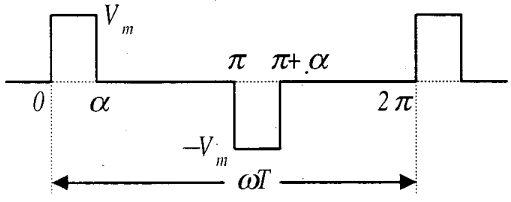

Figure 7 Pulse wave modulation timing

Two different types of the modulation have been examined: a sine wave and a pulse wave modulation (Figure 7), corresponding to various crest factors CF.

In case of a sine wave modulation, the phase currents i_1 and i_2 can be expressed by DC and AC current terms:

$$i_1 = \frac{I_0 + I_m \sin \omega t}{2}$$

$$i_2 = \frac{I_0 - I_m \sin \omega t}{2} . \quad (1)$$

The resultant force at the load is proportional to the difference i_f between phase currents, which has only AC current term.

$$i_f = i_1 - i_2 = I_m \sin \omega t \quad (2)$$

In case of a pulse wave modulation, the phase currents i_1 and i_2 can be also expressed by DC and AC current terms. The resultant force at the load is proportional to the difference i_f between phase currents, which has only AC current term, depending on the particular time interval (Table 1).

$$i_f = i_1 - i_2 \quad (3)$$

Table 1 Pulse wave modulation

time interval	i_1	i_2	i_f
$0 \le \omega t < \alpha$	$\frac{I_0 + I_m}{2}$	$\frac{I_0 - I_m}{2}$	I_m
$\alpha \le \omega t < \pi$	$\frac{I_0}{2}$	$\frac{I_0}{2}$	0
$\pi \le \omega t < \pi + \alpha$	$\frac{I_0 - I_m}{2}$	$\frac{I_0 + I_m}{2}$	$-I_m$
$\pi + \alpha \le \omega t < 2\pi$	$\frac{I_0}{2}$	$\frac{I_0}{2}$	0

The power supply current i_0 for both sine wave and pulse wave modulation is appropriate to the sum of phase currents and has only DC current term independent on time.

$$i_0 = i_1 + i_2 = I_0 \tag{4}$$

The power P_0 generated by the power supply can be derived as follows:

$$P_0 = \frac{1}{T}\int_0^T V_0 i_0 dt = V_0 I_0 \tag{5}$$

where V_0 is the power supply voltage.

The power P_R dissipated by the load in case of a sine wave modulation is derived as

$$P_R = \frac{1}{T}\int_0^T \left(Ri_1^2 + Ri_2^2\right)dt = \frac{RI_0^2}{2} + \frac{RI_m^2}{4} = P_{DC} + P_{AC} \tag{6}$$

while the power P_R dissipated by the load in case of a pulse wave modulation is derived as

$$P_R = \frac{1}{T}\int_0^T \left(Ri_1^2 + Ri_2^2\right)dt = \frac{RI_0^2}{2} + \frac{RI_m^2\alpha}{2\pi} = P_{DC} + P_{AC} \tag{7}$$

where P_{DC} is the DC power and P_{AC} is the AC power. Both sine wave and pulse wave modulation can be handled by the same set of general equations assuming that $\frac{\alpha}{\pi} = \frac{1}{2}$, based on the results obtained in (6) and (7).

The switching bridge efficiency η reduces the portion of the power generated by the power supply, which can be dissipated by the load according to

$$\eta P_0 = P_R \tag{8}$$

$$\eta V_0 I_0 = \frac{RI_0^2}{2} + \frac{RI_m^2\alpha}{2\pi} . \tag{9}$$

After solving the above quadratic equation, DC current I_0 is given by

$$I_0 = \frac{\eta V_0}{R}\left[1 - \sqrt{1 - \frac{\alpha}{\pi}\left(\frac{RI_m}{\eta V_0}\right)^2}\right] . \tag{10}$$

The overall system efficiency η_0 describing both the BBA and its load can be expressed as

$$\eta_0 = \frac{P_{AC}}{P_0} = \frac{\eta}{2}\left[1 + \sqrt{1 - \frac{\alpha}{\pi}\left(\frac{RI_m}{\eta V_0}\right)^2}\right] . \tag{11}$$

Assuming only switch conduction loss due to the ON resistance R_{ON} of the switch, we have

$$V_0 I_0 = \frac{(R + R_{ON})I_0^2}{2} + \frac{(R + R_{ON})I_m^2\alpha}{2\pi} . \tag{12}$$

The switching bridge efficiency η can be derived by dividing (9) with (12).

$$\eta = \frac{R}{R + R_{ON}} \tag{13}$$

The average voltage at the switching bridge output is equal to the half of the bridge capacitor voltage in condition of an unbiased AC modulation signal. The DC voltage loop connecting the power supply with the switching bridge through one load's phase is described by

$$V_0 = \frac{(R + R_{ON})I_0}{2} + \frac{V_C}{2} = \frac{RI_0}{2\eta} + \frac{V_C}{2} . \tag{14}$$

Solving (14) for V_C yields

$$V_C = 2V_0 - \frac{RI_0}{\eta} . \tag{15}$$

Substituting (10) into (15) gives

$$V_C = V_0\left[1 + \sqrt{1 - \frac{\alpha}{\pi}\left(\frac{RI_m}{\eta V_0}\right)^2}\right] . \tag{16}$$

The interesting fact is that the overall system efficiency η_0 can be detected by monitoring the bridge capacitor voltage as follows

$$\eta_0 = \frac{\eta V_C}{2V_0} . \tag{17}$$

The minimum steady-state overall system efficiency $\min\eta_0$ is obtained for maximum steady-state AC current magnitude $\max I_m$ and appropriate maximum steady-state DC current $\max I_0$. In order to derive these limiting values, another set of equations is needed, valid during maximum modulation condition, which still produce undistorted currents and voltages.

A voltage loop connecting the power supply to the ground through single load's phase in the condition of a maximum phase current during maximum modulation is described by

$$V_0 = (R + R_{ON})\frac{(\max I_0 + \max I_m)}{2} = \frac{R(\max I_0 + \max I_m)}{2\eta} . \quad (18)$$

Another voltage loop connecting the power supply with the bridge capacitor through single load's phase in the condition of a minimum phase current during maximum modulation is given by

$$V_0 = (R + R_{ON})\frac{(\max I_0 - \max I_m)}{2} + \min V_C = \frac{R(\max I_0 - \max I_m)}{2\eta} + \min V_C . \quad (19)$$

Subtracting (18) from (19), we obtain the equation for a maximum steady-state AC current:

$$\max I_m = \frac{\eta(\min V_C)}{R} . \quad (20)$$

Adding (18) to (19), and solving for the bridge capacitor voltage, we have

$$\min V_C = 2V_0 - \frac{R(\max I_0)}{\eta} . \quad (21)$$

The simplest way to calculate $\max I_m$ is to multiply equation (18) by $\eta(\max I_0)$, which produces equation (22) and then subtract equation (9) rewritten for the condition of maximum modulation as equation (23):

$$\eta V_0(\max I_0) = \frac{R(\max I_0)^2}{2} + \frac{R(\max I_m)(\max I_0)}{2} \quad (22)$$

$$\eta V_0(\max I_0) = \frac{R(\max I_0)^2}{2} + \frac{R(\max I_m)^2\alpha}{2\pi} . \quad (23)$$

This operation gives direct connection between the maximum steady-state DC and maximum steady-state AC currents:

$$\max I_0 = \max I_m \cdot \frac{\alpha}{\pi} \quad (24)$$

which can be substituted back to the equation (18) in order to derive

$$\max I_m = \frac{\eta V_0}{R} \cdot \frac{2}{1+\frac{\alpha}{\pi}} \quad (25)$$

$$\max I_0 = \frac{\eta V_0}{R} \cdot \frac{2\frac{\alpha}{\pi}}{1+\frac{\alpha}{\pi}} . \quad (26)$$

Now all maximum values can be easily derived by substituting equations (25) and (26) into appropriate equations (7), (11) and (15).

$$\max P_{DC} = 2 \cdot \frac{(\eta V_0)^2}{R} \cdot \left(\frac{\frac{\alpha}{\pi}}{1+\frac{\alpha}{\pi}} \right)^2 \quad (27)$$

$$\max P_{AC} = 2 \cdot \frac{(\eta V_0)^2}{R} \cdot \frac{\frac{\alpha}{\pi}}{\left(1+\frac{\alpha}{\pi}\right)^2} \quad (28)$$

$$\max P_R = 2 \cdot \frac{(\eta V_0)^2}{R} \cdot \frac{\frac{\alpha}{\pi}}{1+\frac{\alpha}{\pi}} \quad (29)$$

$$\min \eta_0 = \frac{\eta}{1+\frac{\alpha}{\pi}} \quad (30)$$

$$\min V_C = \frac{2V_0}{1+\frac{\alpha}{\pi}} \quad (31)$$

Table 2 and Figure 8 shows the efficiency correction $\frac{\eta_0}{\eta}$ for various crest factors CF.

Maximum current through the switch during steady-state (SS) condition is

$$\max I_{SWITCH}|_{SS} = \frac{\max I_0|_{SS} + \max I_m|_{SS}}{2} = \frac{\eta V_0}{R} \quad (32)$$

Table 2 Minimum efficiency correction factor

modulation signal shape	CF	$\frac{\alpha}{\pi}$	$\frac{R\cdot(\max I_m)}{\eta V_0}$	$\frac{\eta_0}{\eta}$
square wave	1	1	1	$\frac{1}{2}$
sine wave	2	$\frac{1}{2}$	$\frac{4}{3}$	$\frac{2}{3}$
pulse wave	$\frac{\pi}{\alpha}$	$\frac{\alpha}{\pi}$	$\frac{2}{1+\frac{\alpha}{\pi}}$	$\frac{1}{1+\frac{\alpha}{\pi}}$
pico pulse	∞	0	2	1

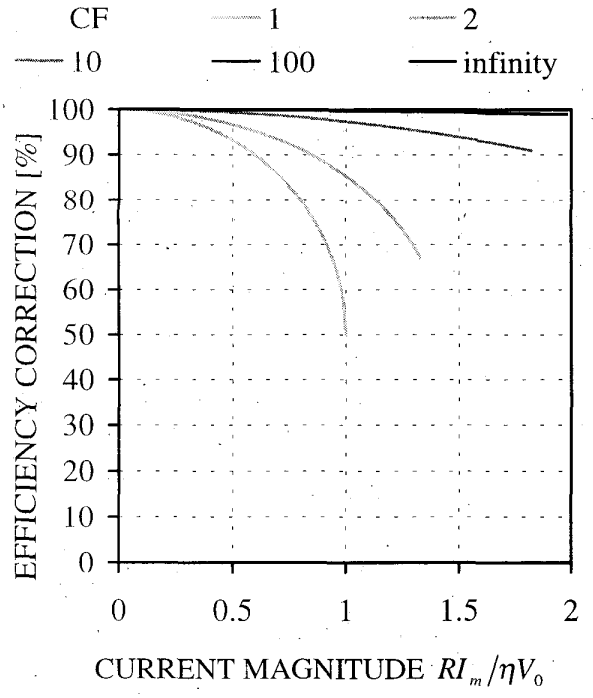

Figure 8 BBA efficiency correction factor

Maximum current through the switch during transient (TR) pulse condition, while bridge capacitor is charged to twice the power supply voltage, is

$$\max I_{SWITCH}\big|_{TR} = \frac{\min I_0\big|_{TR} + \max I_m\big|_{TR}}{2} = \left(0 + \frac{2\eta V_0}{R}\right)\Big/2 = \frac{\eta V_0}{R} . \quad (33)$$

Maximum voltage across the switch during OFF condition is

$$\max V_{SWITCH} = 2V_0 . \quad (34)$$

Maximum bridge capacitor voltage is limited inherently to twice the value of the power supply voltage without using any feedback, in distinction to boost converters where this voltage must be carefully controlled by the negative feedback, in order to avoid switches breakthrough. At the maximum sine wave modulation, the bridge capacitor voltage falls to 4/3 of the power supply voltage, which limits maximum continuous (rms) power to about 2 times greater than the rms power of the CDA, at the same power supply voltage and the same loudspeaker impedance.

On the contrary, in case of a music signal amplification with $10 \le CF < \infty$, rms power is relatively small, so the bridge capacitor voltage reaches almost two power supply voltages. Consequently, a peak power of BBA for a music signal is four times greater than the peak power of CDA with the same power supply voltage and same loudspeaker impedance. At the same time, BBA and CDA efficiencies are practically the same.

4. Experimental results

Automotive grade audio amplifier was built using HIP4080A MOSFET driver, two Si4946 dual 60V N-channel MOSFETs in SO-8 package and various other components for the feedback and protection. Power supply was 14.4V and bridge capacitor value was varied from $100\mu F$ up to $4700\mu F$. Dual 2nd order LC filter with $L = 15\mu H$ and $C = 1.9\mu F$ provided $30kHz$ cut-off frequency.

Simulated BBA timing diagrams are shown in Figure 9 for the pulse wave modulation signal using $C = 1000\mu F$. Experimental timing

diagrams have been almost identical to the simulated in all three cases, thanks to the accurate models for the mentioned power components.

BBA provides the cancellation of current ripple at the switching frequency, thus providing practically DC power supply current i_0 with the superposed small ripple of very low frequency, much below the frequency range of conducted EMI noise limits.

BBA limits the loop with pulse currents to the small area contour connecting the switching bridge and the bridge capacitor, thus dramatically decreasing the radiated emission, and significantly reducing the conducted and radiated EMI noise emanating from the cable connecting the power supply and the loudspeaker. This should be compared to the appropriate loop with pulse currents of CDA, which is closed through an input filter, a cable and the power supply, thus increasing the conducted and radiated EMI noise.

The loudspeaker serves as an additional input filter, eliminating influence of the power supply noise to its own force current. For the perfectly symmetrical phases of the loudspeaker, the theoretical power supply rejection factor (PSRR) is infinite. The experimental PSRR is linearly increasing with frequency from $-85dB$ at $1kHz$ to $-65dB$ at $20kHz$. This solves one of the basic problems of CDA, whose typical PSRR is only $-40dB$ at the end of audio spectrum. The special complicated feedback could increase PSRR up to $-60dB$, which is appropriate to state-of-the-art linear amplifiers in classes A, B and AB. PSRR is very important in car audio where the power supply noise is even greater for the order of magnitude than the power supply voltage itself.

The measurement of total harmonic distortion (THD) was performed using a Pentium PC equipped with the MultiSound Fiji PnP sound card with 56002 DSP and 20-bit A/D and D/A converters supporting $48kHz$ sampling rate. This combination provided satisfactory S/N of $97dB$ within extended audio frequency range from $10Hz$ to $22kHz$. Liberty Audiosuite Ver.3.01 software intentionally rejects all harmonics above $20kHz$ during THD calculation, thus providing step edges on THD diagram when particular harmonics are eliminated from the calculation. However, this approach provides meaningful THD, more appropriate to human capabilities, neglecting harmonics in ultrasonic range, which cannot be heard by any human ear.

Measured total harmonic distortion (THD) for a sine wave modulation within full audio range from $20Hz$ to $20kHz$ at output rms power levels 0.5W, 2W, 8W and 32W is shown in Figure 10 for the $2x2\Omega$ dual resistive load and Figure 11 for the $2x(2\Omega+50\mu H)$ DVC loudspeaker. Similar set of THD diagrams have been obtained from the same amplifier connected in the CDA topology with 28.8V power supply voltage directly connected across the bridge capacitor (Figure 2), and the results have been negligibly different.

In car audio applications with power supply voltage of 14.4V, loudspeaker impedance of 4Ω and distortion of 1%, class AB amplifier achieves 19W rms and 38W peak power, CDA provides 21W rms and 42W peak power, while BBA using $2\Omega+2\Omega$ DVC loudspeaker reaches 42W rms and 193W peak power.

In car audio applications with power supply voltage of 14.4V, loudspeaker impedance of 4Ω and distortion of 10%, class AB amplifier achieves 25W rms and 40W peak power, CDA provides 27W rms and 42W peak power, while BBA using $2\Omega+2\Omega$ DVC loudspeaker reaches 47W rms and 200W peak power.

5. Conclusion

Novel boost bridge amplifier (BBA) utilizing dual-voice coil (DVC) loudspeaker has been theoretically analyzed, simulated, built and tested. According to those results, it follows that BBA is exceptionally adapted to amplify music signals in all battery supplied electronics, such as cars, mobile phones, portable computers, radios, cassette and CD players, etc. Moreover, higher power loudspeakers are already made as DVC, providing that the BBA implementation does not require any change in the state-of-the-art technology of DVC loudspeaker manufacturing.

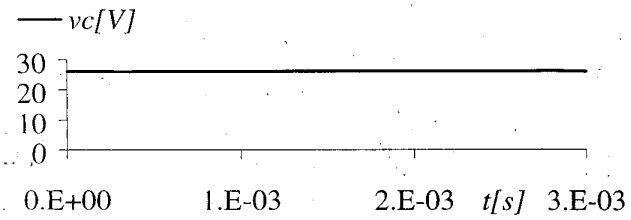

(a) V_C bridge capacitor voltage

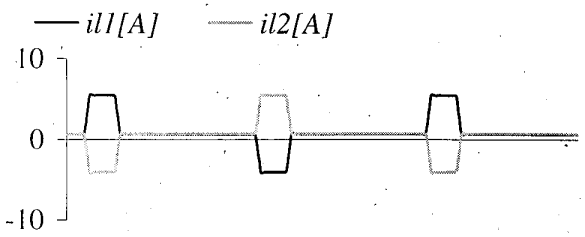

(b) i_{L1} and i_{L2} inductor's currents

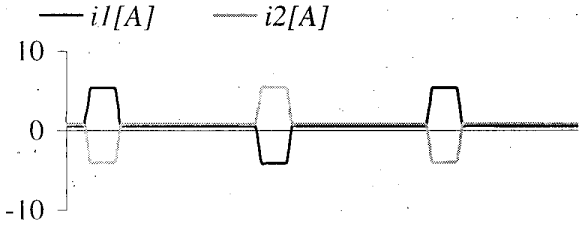

(c) i_1 and i_2 phase currents

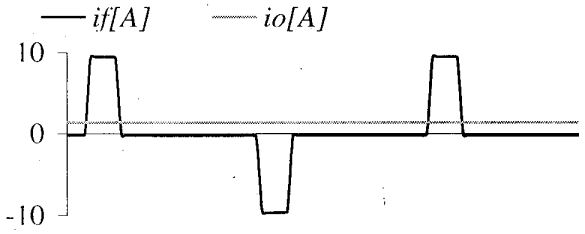

(d) i_f force and i_0 power supply currents

Figure 9 BBA pulse wave timing diagrams

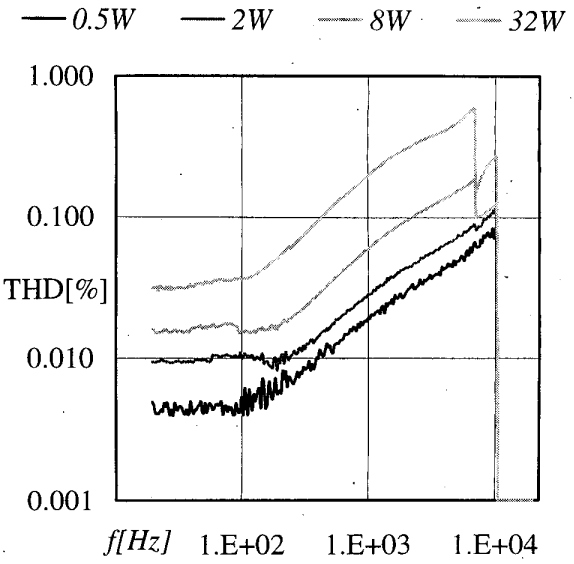

Figure 10 BBA THD with dual resistive load

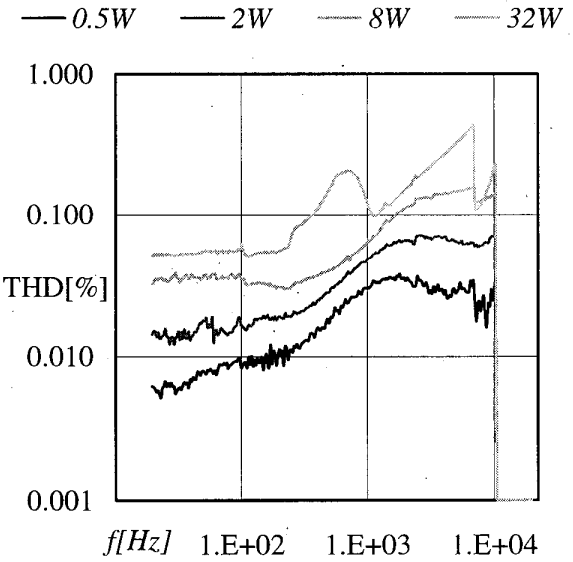

Figure 11 BBA THD with DVC loudspeaker

6. References

[1] D. E. Pauly, "High fidelity switching audio amplifiers using TMOS power MOSFETs," AN1042, Motorola Semiconductor, P.O.B. 20912, Phoenix AZ 85036, USA, 1989.

[2] B. E. Atwood, "Very high fidelity quartz controlled PWM (class-D) stereo amplifiers for consumer and professional use," in *Proc. 59th AES Convention*, Hamburg, Germany, Feb. 28 – Mar. 3, 1978., preprint

[3] B. E. Atwood, "Class-D amplifier system," U.S. Pat. 4,178,556, Dec. 1979.

[4] F. A. Himmelstoss, K. H. Edelmoser and C. C. Anselmi, "Analysis of a quality class-D amplifier," *IEEE Trans. Consumer Electron.*, vol. 42, no. 3, pp. 860-864, Aug. 1996.

[5] J. R. Joseph and W. F. Bleeke, "Digitally driven combination coils for electrodynamic acoustic transducers," U.S. Pat. 4,360,707, Nov. 1982.

[6] B. Choi and B. H. Cho, "Intermediate line filter design to meet both impedance compatibility and EMI specifications," *IEEE Trans. Power Electron.*, vol. 10, no. 5, pp. 583-588, Sep. 1995.

[7] F. A. Himmelstoss and K. H. Edelmoser, "High dynamic class-D power amplifier", *IEEE Trans. Consumer Electron.*, vol. 44, no. 4, pp. 1329-1333, Nov. 1998.

[8] S. Ćuk and R. W. Erickson, "A conceptually new high-frequency switched-mode power amplifier technique eliminates current ripple", in *Proc. of Powercon 5, the Fifth National Solid-State Power Conversion Conference*, San Francisco, CA, USA, May 4-6, 1978.

[9] S. M. Ćuk, "Push-pull switching power amplifier," U.S. Pat. 4,186,437, Jan. 1980.

[10] R. O. Caceres and I. Barbi, "A boost DC-AC converter: analysis, design and experimentation," *IEEE Trans. Power Electron.*, vol. 14, no. 1, pp. 134-141, Jan. 1999.

[11] "A real analysis of the power behind audio power amplifier systems," Texas Instruments Inc., http://www.ti.com, pp. 1-29, 1998.

Biography

Milan Prokin was born in Yugoslavia in 1963. He received the B.S.E.E., M.S.E.E. and Ph.D. degree in 1986, 1988 and 1990, respectively, from Faculty of Electrical Engineering, The University of Belgrade, Yugoslavia.

He joined the Department of Electronics at the same institution in 1986, where he is presently an associate professor. His research areas are switching amplifiers, inverters, real-time control, microcontroller applications and development of advanced I/O devices.